Unexpected Coercivity Enhancement >1T for Nd-Fe-B Permanent Magnets With 20 wt% Nd Produced by Laser Powder Bed Fusion

F. Bittner[1], J. Thielsch[1], and W.-G. Drossel[1,2]

[1]Department of Laser Powder Bed Fusion, Fraunhofer Institute for Machine Tools and Forming Technology, 01187 Dresden, Germany

[2]Institute for Machine Tools and Production Processes, Technical University of Chemnitz, 09111 Chemnitz, Germany

The impact of laser powder bed fusion (LPBF) on coercivity of Nd-lean commercial MQP™-S powder is investigated. It is found that different processing parameters, such as laser power, scan velocity, and hatch spacing, have a remarkable impact on the magnetic performance of LPBF-processed Nd–Fe–B permanent magnets. The increase of energy input during manufacturing will also increase coercivity and a maximum value of 920 kA/m ($\mu_0 H_c$ = 1.15 T) was achieved without any further post-processing. Among other parameters, hatch spacing was identified as the major contribution to coercivity and its role is discussed on basis of the several re-melting events if hatch spacing becomes increasingly smaller than the laser focus diameter. The maximum coercivity is obtained, for hatch spacing of 35 μm and laser focus diameter of 110 μm, which led to a threefold re-melting of the sample.

Index Terms— **Additive manufacturing (AM), coercivity, laser powder bed fusion (LPBF), Nd–Fe–B, permanent magnets.**

I. Introduction

ADDITIVE manufacturing (AM) also called 3-D printing of metallic components by means of laser powder bed fusion (LPBF) is becoming an established processing technology for new complex-shaped products and small series. The benefit of this technology is the high degree of geometrical freedom and short time-to-market. LPBF is currently limited to structural metals and alloys, but also functional materials, such as shape memory alloys or magnetic materials, receive more interest [1]–[3].

The first feasibility studies on LPBF of permanent magnets were published by Kolb *et al.* [4] and Jaćimović *et al.* [5]. The latter obtained bulk magnets from the Nd-lean commercial powder MQP[1]-S [6] with coercivity, H_c, of 695 kA/m, remanence, B_r, of 0.59 T and a maximum energy product, $(BH)_{max}$, of 45 kJ/m^3. Recently, the benchmark for magnetic performance of additively manufactured Nd–Fe–B magnets was enhanced to $(BH)_{max}$ = 63 kJ/m^3 [7]. The composition of the MQP-S powder belongs to the group of $Nd_2Fe_{14}B/\alpha$-Fe nanophase composites [5], [8]. Such materials show a lower coercivity due to the appearance of soft-magnetic α-Fe [8]. However, the achieved coercivity for LPBF-processed Nd–Fe–B magnets using the same premateriial can lie between 886 [7] and 519 kA/m [9]. The aim of this study is to clarify how the LPBF process has to be designed to obtain maximum coercivity without any further post-processing and what are the contributions of different process parameters to it.

Manuscript received 19 March 2021; revised 29 September 2021 and 9 February 2022; accepted 4 April 2022. Date of publication 13 April 2022; date of current version 26 August 2022. Corresponding author: F. Bittner (e-mail: florian.bittner@iwu.fraunhofer.de).

Color versions of one or more figures in this article are available at https://doi.org/10.1109/TMAG.2022.3167246.

Digital Object Identifier 10.1109/TMAG.2022.3167246

[1]Registered trademark.

II. Experimental Part

A. AM by LPBF

LPBF is a layer-by-layer AM technique, which utilizes lasers to selectively melt metal powder and then fuse during solidification.

An LPBF machine is composed of a laser and scanner system, a powder stock, a coater, and a built platform. In the beginning of the process, a thin layer of powder is provided from the powder stock and placed on the built platform by the coater. The laser is moved across the platform by the scanner system to selectively melt the powder. Afterward, the built platform is lowered by a defined value called layer thickness and a new layer of powder is applied by the coater. This process is continued until the complete part is generated.

For this study, we have prepared cylindrical samples (diameter 5 mm and height 5 mm) using a commercial M2 LPBF machine from Concept Laser GmbH, which is equipped with a 400 W diode-pumped fiber laser (wavelength 1070 nm) with a laser spot size of 110 μm. To prevent oxidation, LPBF was performed under Ar atmosphere with an O_2 content below 0.5%. The samples were built on a steel substrate.

To study the impact of the LPBF process on coercivity of additively manufactured Nd–Fe–B permanent magnets, the main process parameters, laser power P_L, scan velocity v_{scan}, and hatch spacing h_y, were varied, whereas the layer thickness z was kept constant at 30 μm. The basic parameter field for the successful fabrication of Nd–Fe–B permanent magnets by LPBF has been discussed elsewhere [7].

The energy impact of the principle process parameters can be quantified by the line energy E_L and volume energy E_V as follows [10]:

$$E_L = P_L / v_{scan} \quad (1)$$

$$E_V = E_L / (h_y \cdot z). \quad (2)$$

Within this study, E_V was varied between 18 and 79 J/mm^3.

B. Materials and Characterization

Spherical Nd–Fe–B powder (MQP-S from Magnequench [6]) was used in this study. The MQP-S powder is called hereafter powder. It was originally designed for the fabrication of polymer-bonded magnets by extrusion and shows a particle size distribution between 10 and 115 μm. The LPBF process requires a powder with a particle size between 10 and 45 μm. For this reason, the material was sieved prior to the LPBF process to the desired fraction.

The density of the LPBF-processed magnets was estimated by measuring the size and mass of the magnets after the LPBF process. We observed a low density of 4.65 g/cm^3 (62.5% of the theoretical density) for E_V of 18 J/mm^3, which increases to 6.77 g/cm^3 (91%) for $E_V = 44$ J/mm^3 and reaches an almost constant value of 6.6 g/cm^3 (89%) for $E_V > 44$ J/mm^3.

The magnetic properties were measured in a closed magnetic circuit using a permeagraph (Magnetphysik GmbH) with a maximum applied field of 1800 kA/m at room temperature.

III. Results and Discussion

The magnetic performance of Nd–Fe–B magnets, which were fabricated by LPBF, depends strongly on the adjusted processing parameter. Fig. 1(a) shows the demagnetization branch of the hysteresis curve for magnets, which were fabricated by increasing volume energy E_V from 18 to 79 J/mm^3.

If the volume energy was too low, e.g., lower than 50 J/mm^3, the demagnetization curve shows some soft magnetic behavior at low reversal fields, which is visible as a step in the demagnetization curve. This behavior is not observed for larger E_V values.

Starting from the lowest E_V value (18 J/mm^3) remanence and coercivity increase remarkably, if E_V is raised. However, for remanence, this effect is limited and an increase above 0.63 T seems not possible. In contrast to this, coercivity is continuously increasing over the full studied range of E_V values. Once the critical E_V of 50 J/mm^3 is exceeded, the demagnetization curve of the LPBF-produced magnets shows the typical appearance of an isotropic permanent magnet without a step at low reversal fields in the demagnetization curve.

The demagnetization curve of the initial powder is added in Fig. 1(a) for comparison. The powder has an apparent remanence of 0.71 T and a coercivity of 710 kA/m. Apparent means that for the unconsolidated powder, a density of 100% is assumed. However, for the fabrication of polymer-bonded magnets from this material, the maximum volume fraction of magnetic material is limited to typically 50%–60% for injection molding (IM) and 70% for compression molding. The reduction of volume fraction for magnetic material will then cause an equivalent decrease in remanence.

Obviously, the coercivity of LPBF-produced magnets can overcome the value of the powder remarkably and the highest observed value within our study is 920 kA/m ($\mu_0 H_c = 1.15$ T).

This enhancement of 30% was not expected, as the initial powder has a rare Earth lean composition of (Nd + Pr) $\approx$ 8 at.% [5], [7].

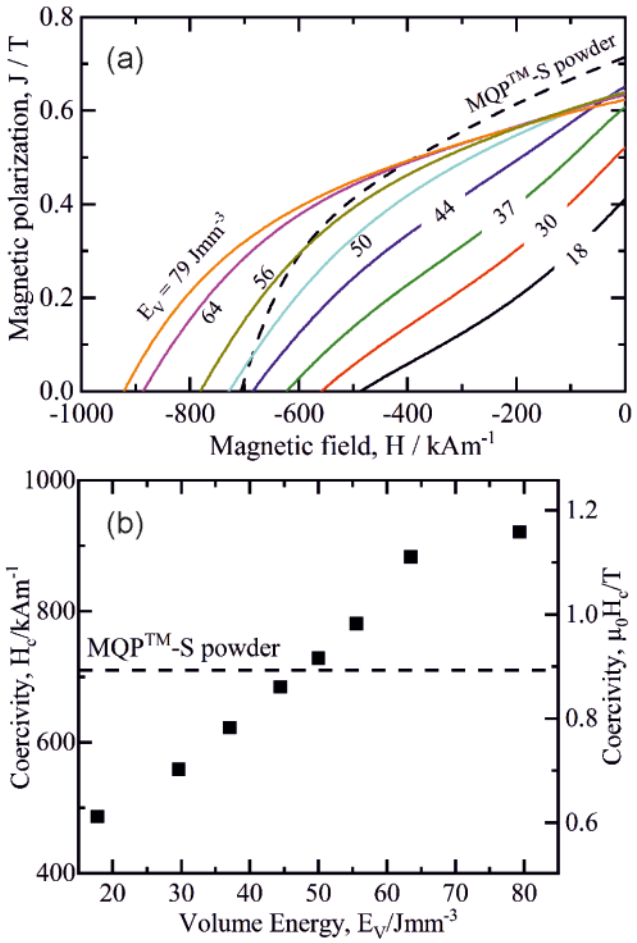

Fig. 1. (a) Demagnetization curves for magnets, which were manufactured by LPBF with volume energies between 18 and 79 J/m^3, and (b) impact of volume energy E_V during LPBF on coercivity H_c.

Fig. 1(b) shows the impact of volume energy on coercivity for LPBF of Nd–Fe–B permanent magnets. Coercivity increases with increasing volume energy between 18 and 64 J/mm^3 almost linear from 486 to 880 kA/m. An increase to $E_V = 79$ J/mm^3 causes only a slight further enhancement of coercivity to 920 kA/m. The reason for this flattening at higher E_V value is the general processability of this material by LPBF as discussed elsewhere [7]: processing with even higher energy input is not possible due to the appearance of extensive cracking and delamination.

According to (2), volume energy depends on different process parameters that were varied within this study except for the layer thickness. Thereby, laser power was adjusted between 50 and 150 W, scan velocity was between 1000 and 2500 mm/s, and hatch distance was 35, 75, and 100 μm. Fig. 2 shows the impact of laser power and scan velocity on coercivity for hatch spacing of 35 μm [Fig. 2(a)] and 75 μm [Fig. 2(b)]. The propagation of coercivity between the experimentally validated parameter combinations is interpolated. An increase of laser power or a reduction of scan velocity or hatch spacing leads to an enhancement of coercivity.

Fig. 3 shows the influence of line energy, i.e., ratio between laser power and scan velocity, on coercivity for different hatch spacing. From the data, a linear relationship between line

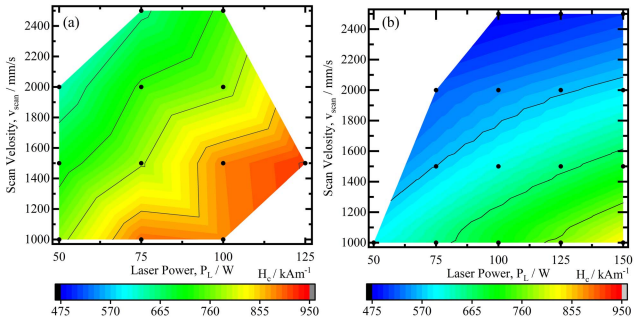

Fig. 2. Impact of laser power P_L and scan velocity v_{scan} on coercivity of Nd–Fe–B permanent magnets produced by LPBF for a hatch spacing of (a) 35 μm and (b) 75 μm. (Note: same color code for both subfigures.)

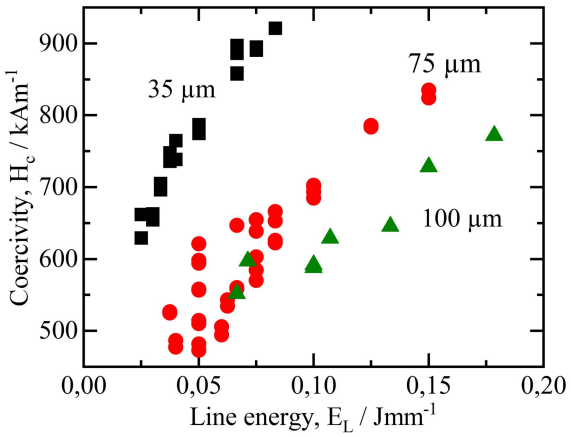

Fig. 3. Impact of line energy E_L on corcivity for different hatch spacings.

energy and coercivity for the applied hatch spacings can be derived. For increasing line energy, coercivity increases too. However, the slope itself depends on hatch spacing. It becomes larger as the hatch spacing decreases. In other words, the enhancement of coercivity is more pronounced for reduced hatch spacing. Furthermore, reduced hatch spacing will always cause a higher coercivity, if line energy is kept constant. The effect of enhancing coercivity by increasing line energy or reducing hatch spacing is limited. In both cases, volume energy will raise. The maximum allowed volume energy for LPBF of Nd–Fe–B permanent magnets is limited for the used combination of laser beam melting machine and RE-lean powder to approximately 80 J/m^3. Exceeding this value will lead to extensive crack formation or delamination [7].

The penetration of a focused laser beam will heat the powder until it melts. The interaction volume, which is called melt pool, has a shape of a spheroid. Distraction of the laser beam by the scanner unit creates a single melt track and leads to the fusion of the powder. If the hatch spacing, i.e., the distance between neighboring tracks, is smaller than the melt track width w_{tr}, two tracks are overlapping. Overlapping means that at least a part of the previously melted and solidified track will be re-heated and re-melted again. This situation is schematically shown in Fig. 4. The fraction of volume, which is re-melted, is given by the ratio of w_{tr}/h_y. If the ratio is <1 no overlapping of melt tracks will appear and

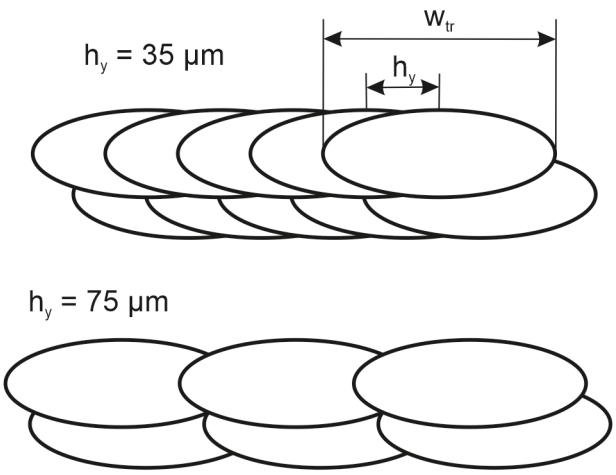

Fig. 4. Schematic illustration of the effect of reduced hatch spacing h_y and melt track width w_{tr} on overlapping of melt pools and re-melting.

TABLE I
COMPARISON OF RESULTS FOR COERCIVITY OF Nd–Fe–B PERMANENT MAGNETS MADE FROM MQP-S POWDER OR SIMILAR RE-LEAN COMPOSITION (IM: INJECTION MOLDING AND MS: MELT SPINNING)

Reference	Material	Processing	Coercivity, H_c
This study	MQP^{TM}-S	LPBF	920 kA/m
Magnequench [6]	MQP^{TM}-S	powder	710 kA/m
Magnequench [6]	MQP^{TM}-S	IM	671 kA/m
Jacimovic et al. [5]	MQP^{TM}-S	LPBF	695 kA/m
Huber et al. [9]	MQP^{TM}-S	LPBF	519 kA/m
Urban et al. [11]	MQP^{TM}-S	LPBF	825 kA/m
Wang et al. [12]	$Nd_9Fe_{84}Zr_1B_6$	MS	630 kA/m

the lack of fusion will create remaining porosity in the final part. On the other hand, for $w_{tr}/h_y > 2$ the whole volume of the part will be melted at least two times.

w_{tr} can be approximated by the spot diameter of the focused laser beam, which is 110 μm in the present case. For a hatch spacing of 75 μm, the ratio w_{tr}/h_y is 1.46. In other words, 50% of the volume is melted twice during LPBF. The ratio increases to 3.1, if the hatch spacing is reduced to 35 μm. In this case, the whole volume is melted three times during LPBF.

The different hatch spacings shown in Fig. 3 will lead to almost no overlapping and re-melting for $h_y = 100$ μm, moderate re-melting at the melt track boundaries for $h_y = 75$ μm, and several re-melting of the whole volume for $h_y = 35$ μm.

Table I summarizes the coercivities of Nd-lean MQP-S powder, which were obtained by various conventional and

AM techniques as well as by our present study. As mentioned above, the powder was originally designed for the fabrication of polymer-bonded magnets by compression molding or IM.

LPBF is characterized by local melting of the powder. This is associated with rapid cooling, whereby cooling rates can be in the order of 10^4–10^5 K/s depending on the adjusted manufacturing parameters [13], [14].

Very different results of coercivity have been reported for different LPBF studies so far. It should be mentioned that the highest value of coercivity for the respective study is given in Table I, which was obtained each by an optimized procedure.

Coercivity of permanent magnets depends on intrinsic magnetic properties, such as anisotropy constant K_u and saturation magnetization M_s, and on microstructure, which includes grain size [15]–[17], defects [18], and other phases [19]. K_u and M_s are predefined by the magnetic phase and its composition, while microstructure is affected by processing.

For this reason, we believe that the microstructure of Nd–Fe–B permanent magnets is largely influenced by the adjusted processing parameter. A modification of the manufacturing process will vary the microstructure and result in different magnetic properties, especially for the microstructure-sensitive coercivity. The microstructural development will be determined by the thermal history of the material. Therefore, melt pool size, cooling rate, and the number of re-meltings are important variables.

Melt spinning is an established rapid cooling technique for the preparation of Nd–Fe–B. Microstructure and resulting coercivity depend in this case primarily on the cooling rate [20], [21]: a low cooling rate, also called under-quenched state, creates a heterogeneous microstructure with a pronounced step in the demagnetization curve. For optimal cooling, the melt spun ribbon consists of a uniform nanocrystalline microstructure and a further increase in cooling rate—also called overquenched state—deteriorates the magnetic properties through increasing amorphization.

For LPBF, an increase in energy input will reduce the cooling rate [14]. The best performance in coercivity was obtained for maximum volume energy in our present study. Therefore, we believe that LPBF with high volume energy, i.e., >60 J/mm^3, is in analogy to melt spinning equivalent to the optimum quenched state. A reduction of volume energy will increase the cooling rate [14] and leads to an overquenched condition. This assumption is supported by recent microstructural investigations of LPBF prepared Nd–Fe–B permanent magnets, which proved a fine microstructure with grain size <1 μm [22]–[24]. Thereby, notable differences in the microstructure for processing with low and high energy inputs were observed [22].

Melt spinning of $Nd_2Fe_{14}B/\alpha$-Fe nanocomposites with comparable rare Earth content results typically in coercivities below 700 kA/m [12], [25]. This value is largely exceeded by the LPBF technique, which emphasizes that there may exist some similarities between melt spinning and LPBF, but further factors LPBF-specific factors, e.g., re-melting by reduced hatch spacing, contribute to high coercivity in this kind of magnets. The clarification of the underlying mechanisms in microstructural development and resulting magnetic properties is object of our further investigations.

IV. Conclusion

Nd–Fe–B permanent magnets with very different magnetic characteristics have been prepared by the AM technology LPBF. Thereby, the volume energy input during manufacturing was varied between 18 and 79 J/mm^3. It was found that the coercivity of LPBF-processed Nd–Fe–B permanent magnets depends strongly on the processing parameter and an unexpectedly high value of 920 kA/m was achieved for a Nd-lean material with only 20 wt% Nd. This value exceeds the one of the initial powder material by 30% and represents the highest value, which was obtained by this material independently of the preparation technique. Our results show that novel manufacturing approaches, such as LPBF, can lead to a substantial improvement in the magnetic performance of Nd–Fe–B permanent magnets.

The complex interplay between local melting by a focused laser beam, rapid cooling, and several re-heating and re-melting is responsible for this improvement and the adjustment of the main process parameters affects the microstructure and resulting magnetic properties.

Acknowledgment

The authors thank the “Fraunhofer Society” for funding within the internal Attract program “InMagMat–Integration of Magnetic Materials by Additive Manufacturing.”

References

[1] S. L. Sing and W. Y. Yeong, “Laser powder bed fusion for metal additive manufacturing: Perspectives on recent developments,” *Virtual Phys. Prototyping*, vol. 15, no. 3, pp. 359–370, Jul. 2020, doi: 10.1080/17452759.2020.1779999.

[2] C. Y. Yap *et al.*, “Review of selective laser melting: Materials and applications,” *Appl. Phys. Rev.*, vol. 2, no. 4, p. 41101, 2015, doi: 10.1063/1.4935926.

[3] V. Chaudhary, S. A. Mantri, R. V. Ramanujan, and R. Banerjee, “Additive manufacturing of magnetic materials,” *Prog. Mater. Sci.*, vol. 114, Oct. 2020, Art. no. 100688.

[4] T. Kolb *et al.*, “Laser beam melting of NdFeB for the production of rare-earth magnets,” in *Proc. 6th Int. Electr. Drives Prod. Conf. (EDPC)*, Nuremberg, Germany, Nov./Dec. 2016, pp. 34–40.

[5] J. Jačimovič *et al.*, “Net shape 3D printed NdFeB permanent magnet,” *Adv. Eng. Mater.*, vol. 19, no. 8, Aug. 2017, Art. no. 1700098, doi: 10.1002/adem.201700098.

[6] *MQP-S-11-9-20001-070 Isotropic Powder Magnequench*. [Online]. Available: https://mqitechnology.com/product/mqp-s-11-9-20001/

[7] F. Bittner, J. Thielsch, and W.-G. Drossel, “Laser powder bed fusion of Nd-Fe-B permanent magnets,” *Prog. Additive Manuf.*, vol. 5, pp. 3–9, Mar. 2020.

[8] G. C. Hadjipanayis, “Nanophase hard magnets,” *J. Magn. Magn. Mater.* vol. 200, pp. 373–391, Oct. 1999.

[9] C. Huber *et al.*, “Coercivity enhancement of selective laser sintered NdFeB magnets by grain boundary infiltration,” *Acta Mater.*, vol. 172, pp. 66–71, Jun. 2019, doi: 10.1016/j.actamat.2019.04.037.

[10] A. Simchi, “Direct laser sintering of metal powders: Mechanism, kinetics and microstructural features,” *Mater. Sci. Eng., A*, vol. 428, no. 1–2, pp. 148–158, Jul. 2006.

[11] N. Urban, A. Meyer, S. Kreitlein, F. Leicht, and J. Franke, “Efficient near net-shape production of high energy rare earth magnets by laser beam melting,” *Appl. Mech. Mater.*, vol. 871, pp. 137–144, Oct. 2017, doi: 10.4028/www.scientific.net/AMM.871.137.

[12] C. Wang, M. Yan, and Q. Li, “Effects of Nd and B contents on the thermal stability of nanocomposite $(Nd,Zr)_2Fe_{14}\beta/\alpha$-Fe magnets,” *Mater. Sci. Eng., B*, vol. 150, no. 1, pp. 77–82, Apr. 2008, doi: 10.1016/j.mseb.2008.02.007.

[13] J. Schilp, C. Seidel, H. Krauss, and J. Weirather, "Investigations on temperature fields during laser beam melting by means of process monitoring and multiscale process modelling," *Adv. Mech. Eng.*, vol. 6, Jan. 2014, Art. no. 217584, doi: 10.1155/2014/217584.

[14] S. Pauly, P. Wang, U. Kuehn, and K. Kosiba, "Experimental determination of cooling rates in selectively laser-melted eutectic Al-33Cu," *Additive Manuf.*, vol. 22, pp. 753–757, Aug. 2018.

[15] R. Ramesh, G. Thomas, and B. M. Ma, "Magnetization reversal in nucleation controlled magnets. II. Effect of grain size and size distribution on intrinsic coercivity of Fe-Nd-B magnets," *J. Appl. Phys.*, vol. 64, no. 11, pp. 6416–6423, Dec. 1988, doi: 10.1063/1.342055.

[16] K. Uestuener, M. Katter, and W. Rodewald, "Dependence of the mean grain size and coercivity of sintered Nd–Fe–B magnets on the initial powder particle size," *IEEE Trans. Magn.*, vol. 42, no. 10, pp. 2897–2899, Oct. 2006, doi: 10.1109/TMAG.2006.879889.

[17] F. Bittner *et al.*, "Normal and abnormal grain growth in fine-grained Nd-Fe-B sintered magnets prepared from He jet milled powders," *J. Magn. Magn. Mater.*, vol. 426, pp. 698–707, Mar. 2017, doi: 10.1016/j.jmmm.2016.10.139.

[18] R. Ramesh and K. Srikrishna, "Magnetization reversal in nucleation controlled magnets. I. Theory," *J. Appl. Phys.*, vol. 64, no. 11, pp. 6406–6415, Dec. 1988, doi: 10.1063/1.342054.

[19] G. Hrkac *et al.*, "Impact of different Nd-rich crystal-phases on the coercivity of Nd–Fe–B grain ensembles," *Scripta Mater.*, vol. 70, pp. 35–38, Jan. 2014, doi: 10.1016/j.scriptamat.2013.08.029.

[20] J. J. Croat, J. F. Herbst, R. W. Lee, and F. E. Pinkerton, "Pr-Fe and Nd-Fe-based materials: A new class of high-performance permanent magnets (invited)," *J. Appl. Phys.*, vol. 55, no. 6, pp. 2078–2082, Mar. 1984.

[21] J. M. Cadogan, D. H. Ryan, and J. M. D. Coey, "Influence of quench rate and hydrogen absorption on the magnetic properties of melt-spun $Nd_{15}Fe_{77}B_8$," *Mater. Sci. Eng.*, vol. 99, nos. 1–2, pp. 143–146, Mar. 1988.

[22] F. Bittner, J. Thielsch, and W.-G. Drossel, "Microstructure and magnetic properties of Nd-Fe-B permanent magnets produced by laser powder bed fusion," *Scripta Mater.*, vol. 201, Aug. 2021, Art. no. 113921.

[23] J. Wu, N. T. Aboulkhair, M. Degano, I. Ashcroft, and R. J. M. Hague, "Process-structure-property relationships in laser powder bed fusion of permanent magnetic Nd-Fe-B," *Mater. Des.*, vol. 209, Nov. 2021, Art. no. 109992.

[24] D. Goll, F. Trauter, T. Bernthaler, J. Schanz, H. Riegel, and G. Schneider, "Additive manufacturing of bulk nanocrystalline FeNdB based permanent magnets," *Micromachines*, vol. 12, no. 5, p. 538, May 2021.

[25] C. Rong and B. Shen, "Nanocrystalline and nanocomposite permanent magnets by melt spinning technique," *Chin. Phys. B*, vol. 27, Nov. 2018, Art. no. 117502.